

## Multispectral Volumetric Curvature Adding Value to 3D Seismic Data Interpretation

Satinder Chopra\*  
Arcis Corp., Calgary, AB, Canada  
schopra@arcis.com

and

Kurt J. Marfurt  
University of Houston, Houston, TX, United States

### Introduction

Computation of volumetric curvature attributes is a significant advancement in the field of attributes. Until recently, curvature attribute applications were limited to interpreted horizons. Horizon-based curvature has been successfully used in the prediction of fault and fractures, and has been shown to be correlated with open fractures measured on outcrops (Lisle, 1994) or measured by production tests (Hart et al., 2002). Horizon-based curvature is limited by the interpreter's ability to pick horizons of interest on 3D seismic data volumes. This could be a challenging task in datasets contaminated with noise and also in zones where rock interfaces do not exhibit significant a consistent impedance contrast to amenable to human interpretation. Very recently, volumetric computation of curvature has been introduced, which dispels the need for consistent horizons in the zone of interest (Al-Dossary and Marfurt, 2006).

An interesting feature of their approach is the multispectral curvature computation that can yield both long wavelength and short wavelength curvature estimates, which enhance geologic features having different scales. Curvature images having different wavelengths provide different perspectives of the same geology (Bergbaueur et al., 2003). Tight (short-wavelength) curvature often delineates details within intense, highly localized fracture systems. Broad (long wavelength) curvature often enhances subtle flexures on the scale of 100-200 traces that are difficult to see in conventional seismic, but are often correlated to fracture zones that are below seismic resolution, as well as to collapse features and diagenetic alterations that result in broader bowls.

Al Dossary and Marfurt (2006) introduced a 'fractional derivative' approach for volume computation of multispectral estimates of curvature. They define the fractional derivative as

$$F_{\alpha} \left( \frac{\partial u}{\partial x} \right) = -i(k_x)^{\alpha} F(k_x),$$

where the operator  $F$  denotes the Fourier transform, where  $u$  is an inline or crossline component of reflector dip, and where  $\alpha$  is a fractional real number that typically ranges between 1 (giving the first derivative) and 0 (giving the Hilbert transform) of the dip. The nomenclature 'fractional derivative' was borrowed from Cooper and Cowans (2003); however, an astute mathematician will note that the  $i$  is not in the parentheses. In this manner we can interpret equation 1 as simply a low pass filter of the form  $kx^{(\alpha-1)}$  applied to a conventional first derivative.

The space domain operators corresponding to different values of  $\alpha$  mentioned above are convolved with the previously computed dip components estimated at every sample and trace within the seismic volume. In addition, the directional derivative is applied to a circular rather than linear window of traces, thereby avoiding a computational bias associated with the acquisition axes. Lower values of  $\alpha$  decrease the contribution of the high frequencies, thereby shifting the bandwidth towards longer wavelength. Thus full 3D curvature attribute volumes are available for analysis at different scales, which helps extract meaningful and subtle information from seismic data.

In Figure 1 we show strat-cube displays of long-wavelength and short-wavelength versions of a fault/fracture system from Alberta. A strat-cube is a sub-volume of seismic data or its attributes, bounded by two horizons which may not necessarily be parallel or covering seismic data above and/or below a given horizon. The surface displayed is close to 1550 ms. Notice, while the long-wavelength display gives the broad definition of such features, the short-wavelength version depicts the finer definition of the individual lineaments.

In Figure 2 we show another comparison of coherence and the most-positive curvature with its long-wavelength and short-wavelength versions. The lineaments seen in the short-wavelength most positive curvature image (Figure 2c) is more detailed than in the coherence (Figure 2a) and the long-wavelength most-positive image (Figure 2b). All attribute interpretations on time and horizon slices should be validated through inspection of the vertical seismic data. In Figure 3 we show a zoomed image of the time slices through coherence, most-positive (both long-wavelength and short-wavelength) and the long-wavelength most-negative curvature volumes intersecting a seismic inline. Notice, how the red peaks (Figure 3b) on the fault lineaments (running almost north-south) correlate with the upthrown signature on seismic. Similarly, the most-negative curvature time-slice intersecting with the seismic inline (Figure 3c) shows the downthrown edges on both sides of the faults highlighted in blue.

## Conclusions

Multispectral volumetric curvature attributes are valuable for prediction of fracture lineaments in deformed strata. Several applications of volume curvature have been completed in different geological settings, which are found to be useful in imaging different stratigraphic features, ranging from channel boundaries, through broad flexures, to small scale faults and highly fractured zones.

## Acknowledgements

We wish to thank Arcis Corporation for permission to publish and present this work.

## References

Marfurt, K. J., 2006: Robust estimates of reflector dip and azimuth: *Geophysics*, 71, P29-P40.  
Bergbauer, S., T. Mukerji, and P. Hennings, 2003, Improving curvature analyses of deformed horizons using scale-dependent filtering techniques: *AAPG Bulletin*, 87, 1255-1272. Cooper, G. R. J., and D. R. Cowans, 2003, Sunshading geophysical data using fractional order horizontal gradients, *The Leading Edge*, 22, 204-205.

Edge, 22, 204-205.

Hart, B.S., R. Pearson, R. Pearson, and G. C. Rawling, 2002, 3-D seismic horizon-based approaches to fracture-swarm sweet spot definition in tight-gas reservoirs: *The Leading Edge*, 21, 28-35.

Lisle, R. J., 1994, Detection of zones of abnormal strains in structures using Gaussian curvature analysis: *AAPG Bulletin*, 78, 1811-1819.

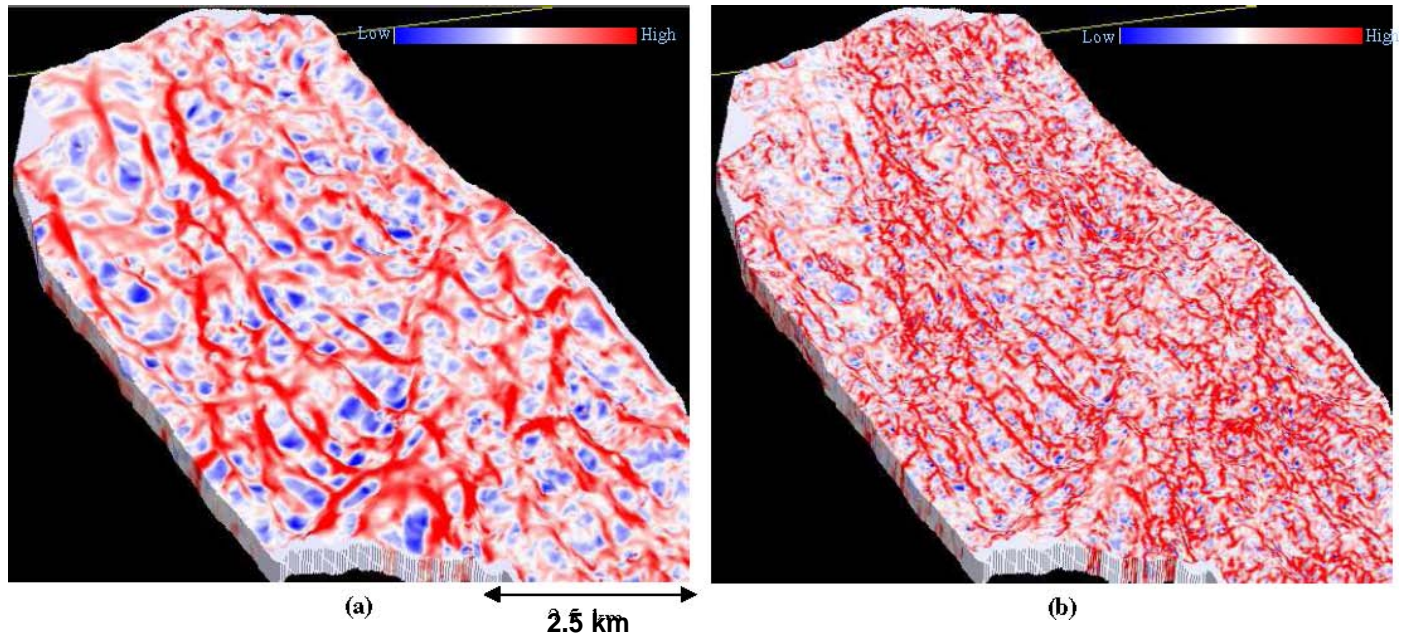


**Figure 1.** Comparison of (a) long-wavelength and (c) high-resolution most-positive curvature strat-cube displays from a 3D volume from Alberta. The finer detail in terms of fault/fracture lineaments could be useful for certain objectives. The upper surface is close to 1550 ms.

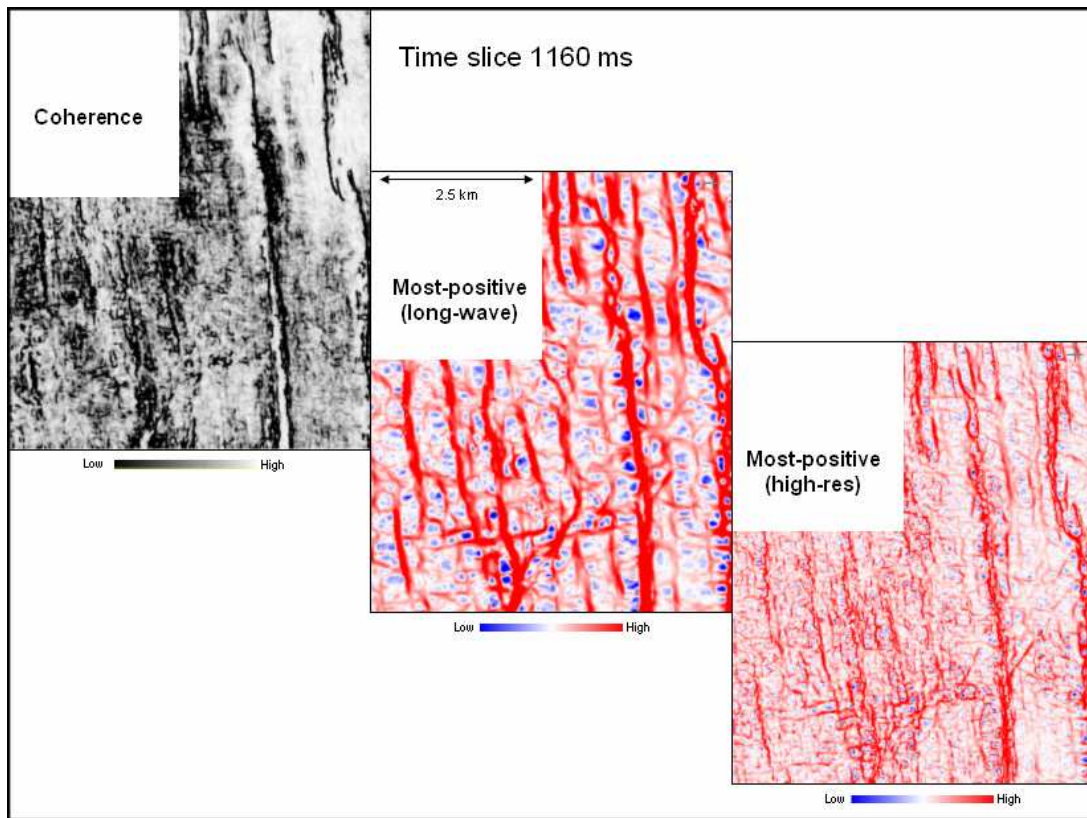


**Figure 2.** Comparison of (a) coherence (b) most-positive curvature (long-wavelength) and (b) most-positive curvature (shortwavelength) horizon slice displays from a 3D volume from Alberta.

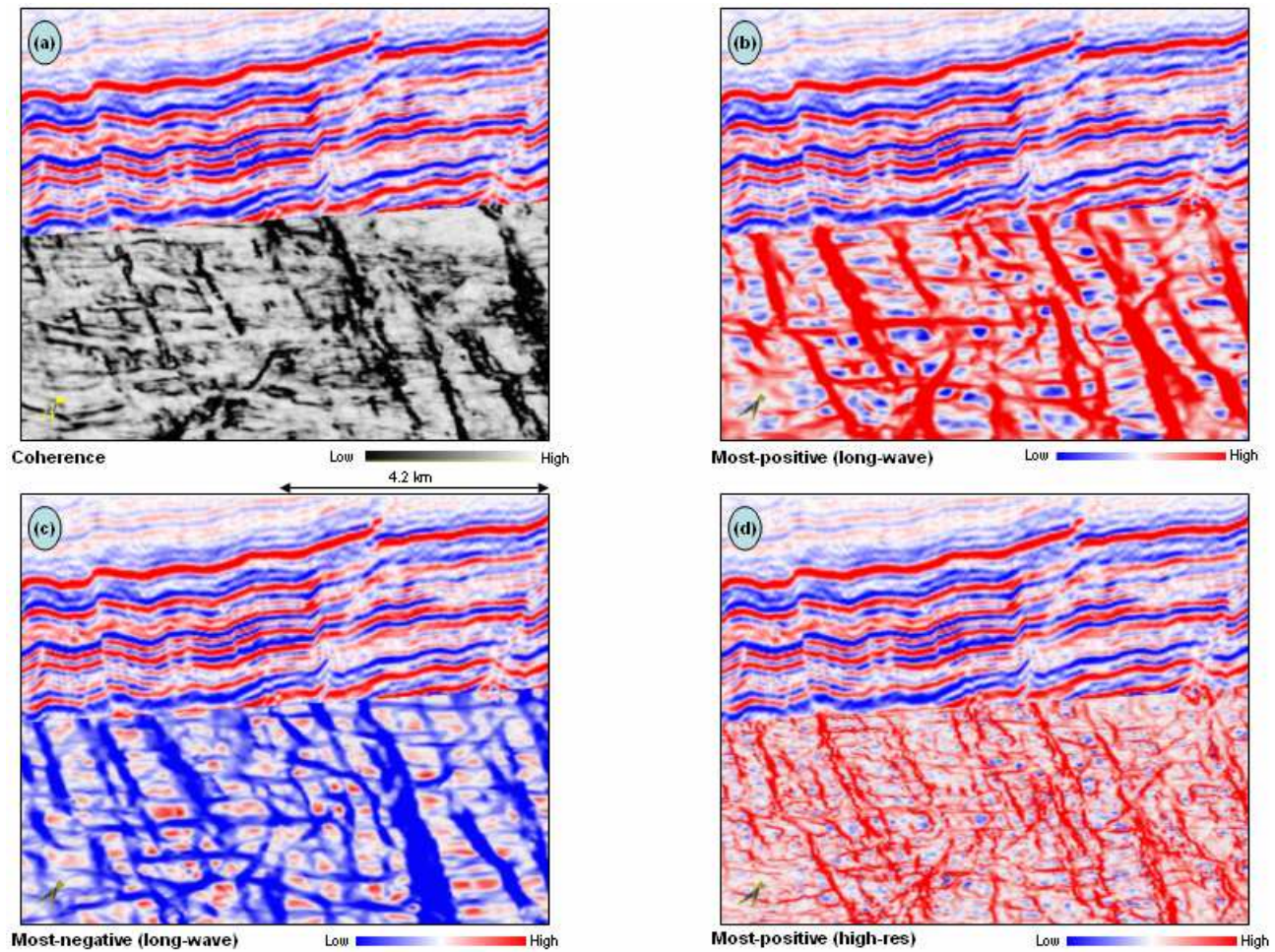


**Figure 3.** Zoom of chair-displays where the vertical display is an inline from the 3D seismic volume and the horizontal displays are time slices through (a) coherence (b) most-positive (long-wavelength) (c) most-negative (long-wavelength) (d) most-positive (shortwavelength) curvature attribute volumes. Note how the fault lineaments correlate with the upthrown and downthrown signatures on the seismic.